



Effects of non-Gaussian noise near supercritical Hopf bifurcation

Ruiting Zhang, Zhonghuai Hou^{*}, Houwen Xin

Hefei National Laboratory for Physical Sciences at Microscales & Department of Chemical Physics, University of Science and Technology of China, Hefei, Anhui 230026, China

ARTICLE INFO

Article history:

Received 8 April 2010

Received in revised form 17 August 2010

Available online 8 October 2010

Keywords:

Hopf bifurcation

Non-Gaussian noise

Noise induced oscillation

Stochastic normal form

ABSTRACT

We have studied the effects of non-Gaussian colored noise in a chemical oscillation system, the well-known Brusselator model, in the parameter region close to the supercritical Hopf bifurcation. With the variation of the parameter q , which quantifies the deviation from Gaussian character, the signal-to-noise ratio of noise induced oscillation exhibits a bell-shaped change, indicating the presence of resonant activity. The cooperative effects of q and the correlation time τ on the performance of noise induced oscillation are also investigated. Interestingly, resonance-like behavior can be induced by either q or τ when the other parameter is properly fixed. Stochastic normal form theory is used to analyze these nontrivial effects and the simulation results are well reproduced. This work provides us comprehensive understanding of how non-Gaussian noise influences the dynamics in chemical oscillation systems.

© 2010 Published by Elsevier B.V.

1. Introduction

In the past two decades, constructive roles played by noise in nonlinear systems have gained considerable attention [1–3]. Of the most interest are the so-called stochastic resonance (SR) and related phenomena. The fingerprint of SR is that the system's response to a feeble input signal, often characterized by some well-defined signal-to-noise ratio (SNR), shows one or more clear-cut peaks as a function of the noise intensity. Albeit it was first introduced in a bistable system to account for the earth's periodic climate change [4,5], SR has found its applications in many other types of dynamical systems. Specifically, in systems with oscillatory or excitable dynamics, noise can induce stochastic oscillations even outside the deterministic oscillatory region, and the SNR of the noise induced oscillation (NIO) shows a bell-shaped dependence on the noise intensity, indicating the occurrence of coherence resonance (CR) [2,6]. In excitable systems such as neurons, NIO is of relaxation type with large amplitude [7,8], while in systems where oscillation results from supercritical Hopf bifurcation (SHB), NIO is harmonic and has small amplitude [9–11]. In systems where SHB and excitability coexist, both types of NIO can be observed [12,13].

In most previous studies, noises were usually assumed to be Gaussian. However, some recent experimental results in sensory systems, particularly for one kind of crayfish [14] and rat skin [15], offer strong implications that noise source could be non-Gaussian and bounded [16–19] in distribution. Recently, effects of non-Gaussian noise (NGN) in nonlinear systems have attracted growing attention [20–33]. It was demonstrated both experimentally [20] and theoretically [21] that SR in a bistable system can be enhanced by NGN [21], and there is a regime in which a notable robustness against noise tuning exists [23]. For Brownian motors driven by NGN, both current and efficiency can be enhanced due to the non-Gaussian character of noise [25,26], and maximal current could be observed when the noise deviates from Gaussian behavior [31]. CR in coupled Hodgkin–Huxley neurons can also be enhanced significantly in the presence of NGN [32,33]. Besides these, the effects of NGN on noise induced transition [24], resonant activation [27] and many other nonlinear dynamical phenomena [28–30] have also been studied. Nevertheless, the effect of NGN near SHB has not been studied so far.

^{*} Corresponding author.

E-mail address: hzhlj@ustc.edu.cn (Z. Hou).

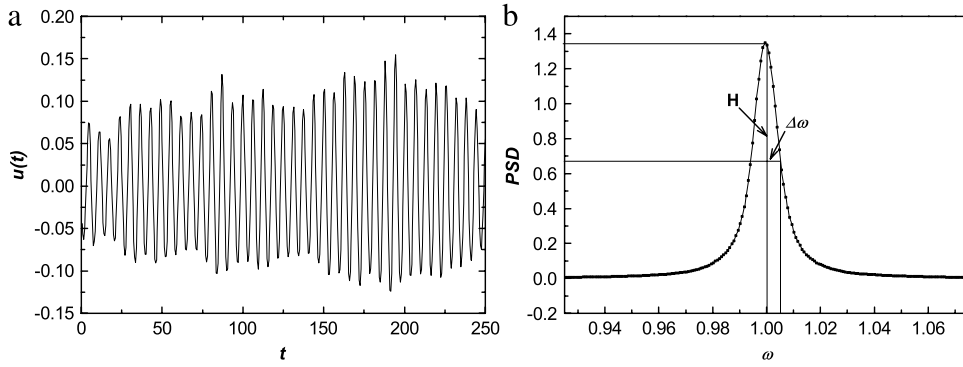


Fig. 1. (a) Typical time series and (b) power spectrum density for non-Gaussian noise induced oscillation. Parameters are $D = 1E-4$, $q = 0$, $\tau = 0.01$.

In this paper, we have studied the effects of NGN near SHB in a well-known chemical oscillation system, the Brusselator model. The NGN is defined by three parameters, D the noise intensity, τ the correlation time and q the quantity characterizing the non-Gaussian distribution. The system's parameters lie in the sub-threshold region where no sustained oscillation exists in the absence of noise. If noise is present ($D \neq 0$), NIO can be observed as expected. We first investigate the SNR of the NIO as functions of D , τ and q numerically. Since we are interested in the non-Gaussian features of the noise, we fix the noise intensity D and let q and τ vary. We find that SNR shows a maximum with the variation of q if τ is smaller than a certain value τ_c , while it increases monotonically with q if $\tau > \tau_c$. On the other hand, SNR shows a maximum with τ if q is larger than some q_c and decreases monotonically with τ if $q < q_c$. Such a scenario is robust to the change of D , except for changes in the location of SNR maxima and the values of τ_c and q_c . Therefore, NGN with moderate q and small τ seems to be most favorable to NIO.

To get a thorough understanding of these nontrivial results, we have used the stochastic normal form theory (SNFT) we developed recently [34–37]. According to SNFT, the SNR is determined by an effective noise intensity σ wherein the power spectrum of the noise plays the key role. We demonstrate that SNFT reproduces the simulation results qualitatively well. The theoretical analysis also provides us clear understanding of how the non-Gaussian feature and noise correlation influence the NIO in a cooperative way.

The paper is organized as follows. The model is presented in Section 2. Simulation results are given in Section 3. We use SNFT to interpret the simulation results in Section 4, followed by conclusions in Section 5.

2. Model description

We consider the conceptual model for chemical oscillations, the Brusselator. The dynamics of the Brusselator system is described by the following equations,

$$\dot{x} = A - (B + 1)x + x^2y + \eta(t) \quad (1a)$$

$$\dot{y} = Bx - x^2y \quad (1b)$$

where $\eta(t)$ denotes the NGN defined via

$$\frac{d\eta(t)}{dt} = -\frac{1}{\tau} \frac{d}{d\eta} V_q(\eta) + \frac{1}{\tau} \xi(t). \quad (2)$$

Herein $\xi(t)$ is a Gaussian white noise with $\langle \xi(t) \rangle = 0$, and $\langle \xi(t)\xi(t') \rangle = 2D\delta(t - t')$, and the distribution function $V_q(\eta)$ is defined as

$$V_q(\eta) = \frac{D}{\tau(q-1)} \ln \left[1 + \frac{(q-1)\tau\eta^2}{2D} \right]. \quad (3)$$

Taking the limit $q \rightarrow 1$, $\eta(t)$ converges to the standard Gaussian colored noise generated by linear Ornstein–Uhlenbeck (OU) process. In addition, for $q < 1$, $V_q(\eta)$ is only well defined in a region $|\eta| < \sqrt{2D/(\tau(1-q))}$, while for $q > 1$, the distribution is wider than Gaussian. Since the second moment of $\eta(t)$ diverges for $q > 5/3$, q can only be chosen between $-\infty$ and $5/3$ to admit a well-defined NGN.

In the absence of noise, Eq. (1) has a fixed point ($x_s = A$, $y_s = B/A$) which loses stability when the control parameter B bypasses the SHB point $B_c = 1 + A^2$ from below. Throughout this study, we fix $A = 1$, $B = 1.996$ so that the system lies in the sub-threshold region. Eqs. (1) and (2) are integrated by using Euler methods with a time step 0.001. The power spectrum density (PSD) of time series $u(t) = x(t) - x_s$ is calculated, from which one can obtain the SNR. In Fig. 1, we show an example of $u(t)$ and the corresponding PSD for $D = 1E-4$, $q = 0$, $\tau = 0.01$. The PSD curve shown in Fig. 1(b) is obtained by Fourier transformation of the auto-correlation function of $u(t)$ with 16 384 data points and then averaging over 200 independent runs. To obtain the SNR, we divide the peak height H by its width $\Delta\omega$ at $H/2$.

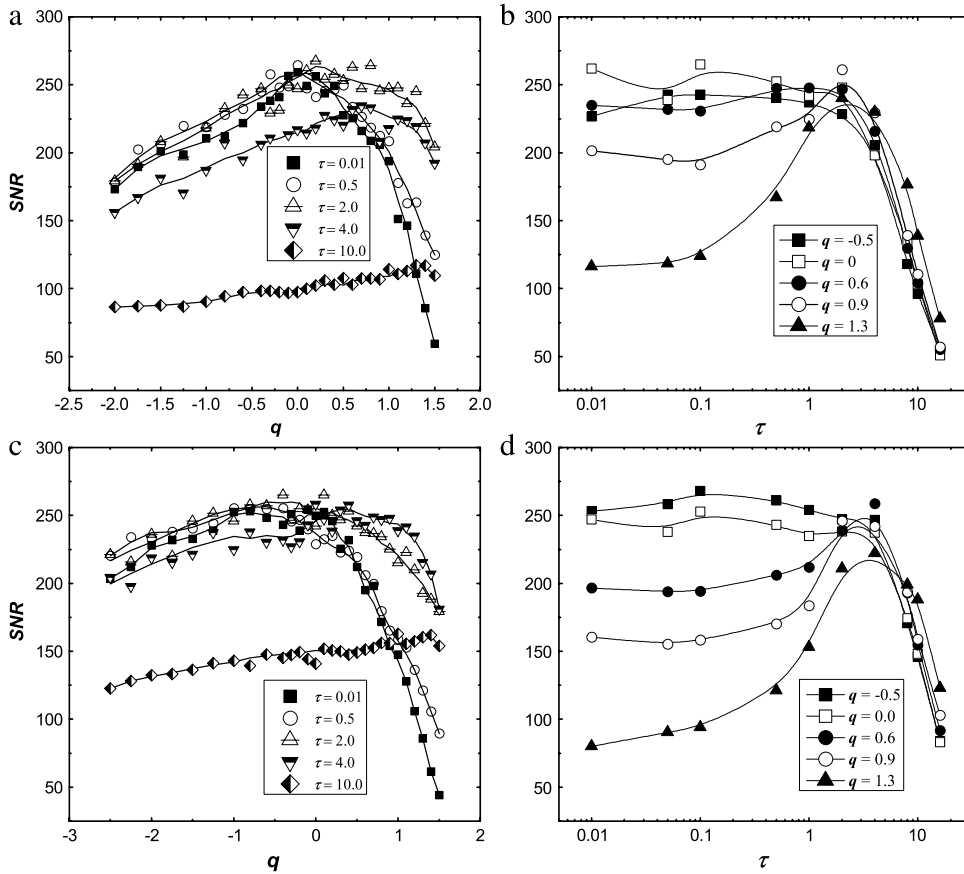


Fig. 2. (a), (c) SNR plotted as functions of q for different correlation time τ . (b), (d) SNR plotted as functions of τ for different values of q . Lines are drawn to guide the eyes. (a), (b), $D = 1E-4$; (c), (d), $D = 2E-4$.

3. Numerical results

In the present study, we mainly focus on how the non-Gaussian features of noise would influence the performance of NIO. To this end, we fix the noise intensity D and vary the parameters q and τ . In Fig. 2(a), SNR are plotted as functions of q for different τ with $D = 1E-4$. Interestingly, SNR shows a clear maximum at a certain $q = q_m$ if τ is not large. With increasing τ , the maximum value of SNR remains nearly unchanged, but the value of q_m becomes larger. If τ is large enough, e.g., $\tau = 10$, q_m moves out of the considered range of $q (< 5/3)$, and in this case, SNR is a monotonically increasing function of q . The crossover from non-monotonic to monotonic behavior takes place at a relative large τ_c . In Fig. 2(b), we show how SNR depends on τ for fixed values of q . This time, the SNR curve shows a peak at $\tau = \tau_m$ if q is larger than a critical value q_c , otherwise SNR decreases with τ . These observations demonstrate that the distribution and correlation of the NGN work in a nontrivial and cooperative way to tune the performance of NIO. NGN with moderate q and small τ seems to be most favorable to NIO. We have also investigated how these results depend on the noise intensity. In Fig. 2(c) and (d), similar plots as those in Fig. 2(a) and (b), respectively, are drawn for $D = 2E-4$. Obviously qualitative features are nearly the same, except that the detailed values of q_m , q_c , τ_m and τ_c change. However, a remarkable feature is that the overall maximum value of SNR remains nearly constant (about 250 shown here) no matter how D , q or τ changes.

4. Theory

To get more insight into the above findings, we turn to the SNFT developed in our recent works [34–37]. Generally, the motivation of normal form computation is to reduce the system dimensionality as much as possible, by some suitable near-identity nonlinear variable transformation, while retaining the essential dynamic characteristics near the critical point. The crucial step is to find the so-called ‘resonant’ terms which cannot be eliminated through the variable transformation. We note here that stochastic normal forms of oscillation systems with Hopf bifurcation have gained a lot attention in the past two decades [38–43]. In the seminar paper of Couillet et al. [38], it was reported that new stochastic resonant terms appear which are absent in the deterministic normal form. Arnold and coworkers have setup rigorous mathematical basis for stochastic normal forms [40,42,44] and have applied them to study the dynamics of the stochastic Duffing–van der Pol oscillator.

Very recently [43], Roberts has performed time-dependent normal form transforms to separate fast and slow modes in stochastic dynamical systems, including the Duffing oscillator. However, NIO and CR were not considered in these studies.

The development of our SNFT contains two main steps. In the first step, we obtain the stochastic normal form near the SHB following similar procedures as that proposed by Arnold [40]. To address the NIO and CR, we only need to keep the terms to the lowest order of noise intensity. In the second step, we use stochastic averaging method [45,46] to approximate the system dynamics by effective Markovian process in the long time limit, resulting in normal form equations that are solvable. This is feasible thanks to the fact that the time evolution of θ is much faster than that of r , where θ and r are the oscillation phase and amplitude, respectively, given that the system is close to the SHB. For more details of our SNFT, please turn to Ref. [34–36].

For the Brusselator system, the complex amplitude of oscillation $Z = ie^{i\theta}$ could be easily obtained from the original variables x and y via the following transformation

$$x = x_s + r \cos \theta, \quad y = y_s - \left(1 + \frac{\alpha}{A^2}\right) r \cos \theta - \frac{\omega_0}{A^2} r \sin \theta \quad (4)$$

where $\alpha = (B - B_c)/2$ measures the distance to the SHB and $\omega_0 = \sqrt{A^2 - \alpha^2}$ is the characteristic frequency at the SHB. When $\alpha \ll 1$, the stochastic normal form equations for variables r and θ read

$$\frac{dr}{dt} = \alpha r + C_r r^3 + \eta_1(t) \quad (5a)$$

$$\frac{d\theta}{dt} = \omega_0 + C_i r^2 + \frac{\eta_2(t)}{r}. \quad (5b)$$

Here, C_r and C_i are constants derived from the nonlinear terms of the system. For the Brusselator model with $A = 1$, $C_r = -3/8$ and $C_i = -1/24$, respectively. The new noise terms are $\eta_1 = \sqrt{1 + A^2} \sin(\theta + \phi)\eta(t)$ and $\eta_2 = \sqrt{1 + A^2} \cos(\theta + \phi)\eta(t)$ with $\phi = \arctg(1/A)$. It is apparent that r and θ are coupled via the stochastic terms, which makes it hard to solve Eqs. (5) directly. However, when the system is very close to the SHB and the noise intensity is small, it is possible to reduce these equations to decoupled ones by using the stochastic averaging method, which read

$$\frac{dr}{dt} = \left(\alpha r + C_r r^3 + \frac{\sigma^2}{2r}\right) + \sigma \eta_r(t) \quad (6a)$$

$$\frac{d\theta}{dt} = (\omega_0 + C_i r^2) + \frac{\sigma}{r} \eta_\theta(t) \quad (6b)$$

where $\eta_r(t)$ and $\eta_\theta(t)$ are two independent Gaussian white noises and σ denotes an effective noise intensity which is proportional to the power spectrum $S(\omega_0)$ of the noise (see the appendix in Ref. [36]),

$$\sigma = \frac{1 + \omega_0^2}{2} \int_{-\infty}^{\infty} \langle \eta(0)\eta(s) \rangle e^{-i\omega_0 s} ds. \quad (7)$$

According to Eq. (6a), the stationary distribution of r exhibits a single peak at the most probable amplitude r_m , which is given by

$$r_m = \left(\frac{\alpha + \sqrt{\alpha^2 - 2C_r \sigma^2}}{-2C_r} \right)^{1/2}. \quad (8)$$

Substituting r_m into Eq. (6b), we can solve the dynamics of $\theta(t)$ and calculate the auto-correlation function $C(\tau) = \langle u(t)u(t + \tau) \rangle$, where $u(t) = r(t) \cos \theta(t)$ and $\langle \cdot \rangle$ stands for averaging over time and noise realizations. By performing Fourier transformation of $C(\tau)$, one gets the PSD, which has a Lorentzian form $\text{PSD}(\omega) \simeq \frac{r_m^2 \tau_c}{1 + (\omega - \omega_1)^2 \tau_c^2}$, where $\tau_c = 2r_m^2/\sigma^2$ and $\omega_1 = \omega_0 + C_i r_m^2$ are auto-correlation time and frequency of the NIO, respectively. Obviously, $\text{PSD}(\omega)$ has a peak at ω_1 with height $H = r_m^2 \tau_c$ and half height width $\Delta\omega = 1/\tau_c$. Then the analytical form of SNR can be obtained :

$$\text{SNR} = \frac{H}{\Delta\omega} = \frac{4r_m^6}{\sigma^4}. \quad (9)$$

By setting $\frac{\partial(\text{SNR})}{\partial(\sigma^2)} = 0$, we can get the optimal effective noise intensity

$$\sigma_{\text{opt}}^2 = \frac{4\alpha^2}{(-C_r)}, \quad (10)$$

and correspondingly the maximum SNR is

$$(\text{SNR})_{\text{max}} = \frac{1}{4\alpha C_r}. \quad (11)$$

From Eqs. (7) and (8), it is clear that what really matters is σ since both α and C_r are constants. As long as one can obtain the auto-correlation function $C_q(s) = \langle \eta(0)\eta(s) \rangle$ of the noise, SNR can be readily calculated theoretically. However, getting

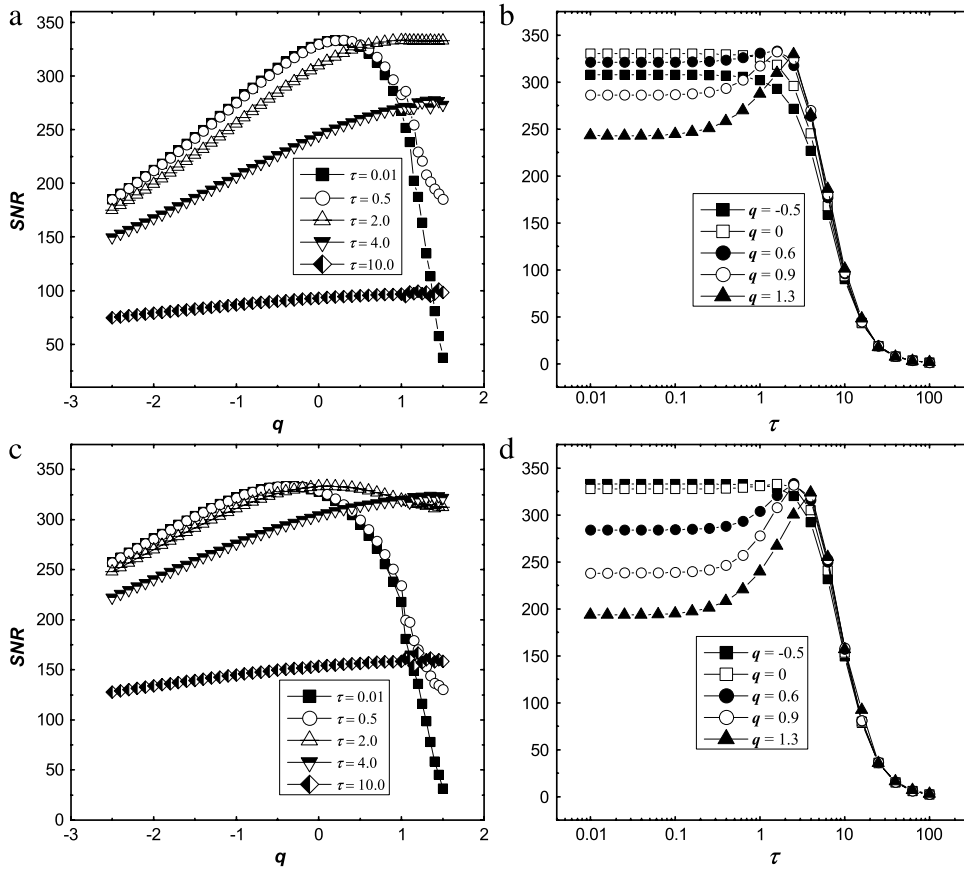


Fig. 3. The theoretical result of SNR is presented in the same parameter region with Fig. 2. (a), (c) SNR plotted as functions of q for different correlation time τ . (b), (d) SNR plotted as functions of τ for different values of q . (a), (b), $D = 1E-4$; (c), (d), $D = 2E-4$.

the analytical expression for $C_q(s)$ is not trivial. By using path integral approach and effective Markovian approximation, Fuentes et al. [22] showed that for $q \leq 1$, $C_q(s)$ is an exponentially decayed function,

$$C_q(s) = \frac{D}{\tau \beta_q} e^{-\frac{\beta_q}{\tau} s} \tag{12}$$

where $\beta_q = \frac{2}{5-3q}$. Thus we can use Eq. (7) to get the analytical form of σ for $q \leq 1$,

$$\sigma^2 = \frac{8D}{4\tau^2 \omega_0^2 + (5 - 3q)^2}. \tag{13}$$

For $q > 1$, the self-correlation function of $C_q(s)$ has the form,

$$C_q(s) = \left[1 + (q - 1) \frac{s}{s_q} \right]^{\frac{1}{1-q}} \tag{14}$$

where $s_q = \int_0^\infty ds C_q(s)$ is the characteristic correlation time. Unfortunately, it is hard to achieve the analytical form of σ from Eq. (14). Hence in this case ($q > 1$), we calculate the SNR numerically from Eqs. (7)–(9) and (14).

According to Eqs. (10) and (11), σ_{opt} and $(SNR)_{max}$ depend only on system parameters C_r and α . For given A and B , C_r and α are both constants. Therefore, tuning q and τ will not change the overall maximal SNR, which was demonstrated in the simulation results. From Eqs. (8) and (9), we notice that the SNR is a bell-shaped function of effective noise σ^2 , which can be adjusted by varying q and τ . If σ bypass σ_{opt} as q increases, the SNR will pass through a maximum at σ_{opt} . For instance, in the case of $q < 1$, σ^2 is given by Eq. (13). For fixed D and τ , increasing q will rise σ^2 monotonically. Note that the maximal value that σ^2 can reach is given by $\sigma_1^2 \equiv 2D/(\tau \omega_0)^2$. Therefore, if $\sigma_{opt} < \sigma_1$, σ can bypass σ_{opt} as q increases, which will lead to the resonance-like phenomenon. The optimal value q_m satisfies $(5 - 3q_m)^2 + 4\tau^2 \omega_0^2 = 8D/\sigma_{opt}^2$. Clearly, q_m becomes bigger with increasing τ . When τ is larger than $\tau_c = \sqrt{2D/\sigma_{opt}^2 \omega_0^2}$, there will be no peak in the SNR curve. Such theoretical

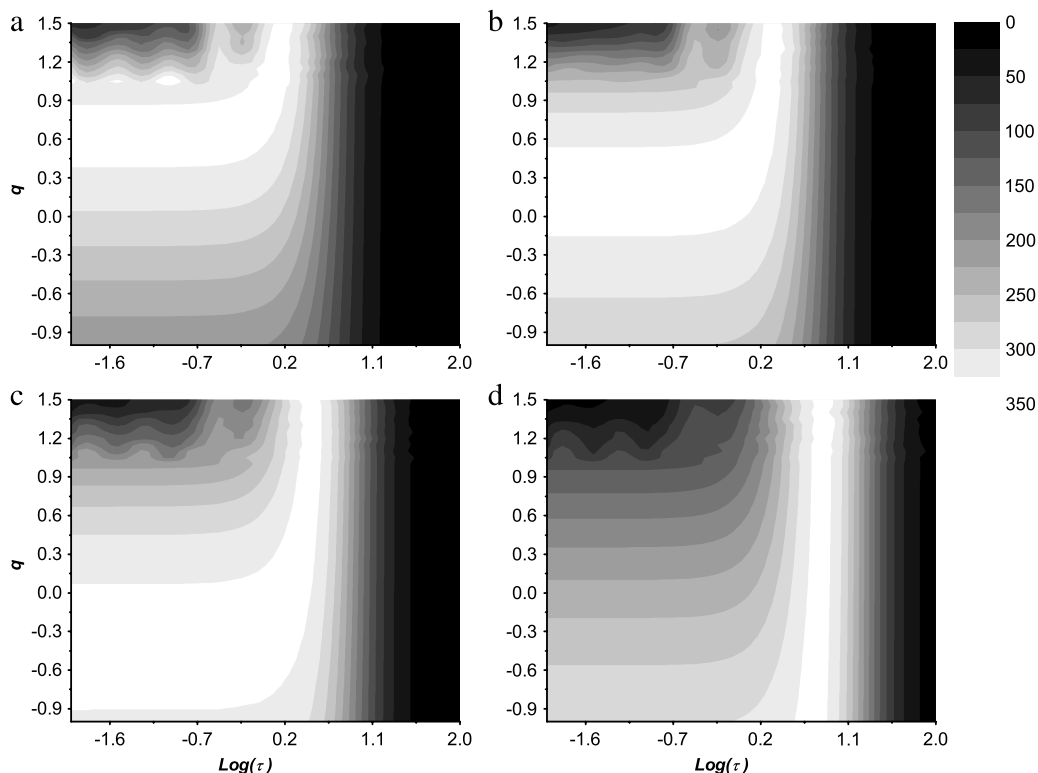


Fig. 4. From (a) to (d), the contour of the SNR is plotted as function of q and correlation time τ . (a) $D = 5E-5$; (b) $D = 1E-4$; (c) $D = 2E-4$; (d) $D = 1E-3$. The SNR is larger in brighter regions.

predictions are in good agreement with the simulations shown in Fig. 2(a) and (c). On the other hand, σ^2 is a monotonically decreasing function of τ for fixed D and q . In this case, SNR will bypass a maximum only when $\sigma_{\text{opt}}^2 < \sigma_2^2 \equiv 8D/(5-3q)^2$. If q is smaller than some threshold value q_c , satisfying $\sigma_{\text{opt}}^2 \equiv 8D/(5-3q_c)^2$, σ^2 and hence SNR will decrease monotonically with τ . These predictions are also consistent with the simulation results in Fig. 2(b) and (d). In Fig. 3, theoretical SNR values are presented, where the parameter regions are the same as in Fig. 2. As expected, the main characters observed in Fig. 2 are well reproduced.

In Fig. 4, contour plots of SNR in $\tau \sim q$ parameter plane are shown. From Fig. 4(a) to (d), the noise intensity is $D = 5E-5$, $D = 1E-4$, $D = 2E-4$ and $D = 1E-3$, respectively. q is between -1 and 1.5 , τ is between 0.01 and 100 . Brighter regions in the figures correspond to larger SNR values. The brightest region forms an ellipse around the upper-left corner of the plane. This region shifts to larger correlation time τ and smaller q when noise intensity D increases. This indicates that at larger noise intensity, regularity of the time series is better in the parameter region where the noise has narrower distribution and smaller correlation time. These contour plots give us a global picture on how τ and q work in a cooperative way in tuning the performance of NIO.

5. Conclusions

In this article, we have studied the effects of non-Gaussian colored noise in the Brusselator model that is near Hopf bifurcation. The non-Gaussian noise is characterized by parameter q , which measures the departure from Gaussian distribution, and the correlation time τ . It is noted that the performance of non-Gaussian noise induced oscillations, quantified by a well-defined SNR, exhibits nontrivial dependence on both q and τ . Moreover, we find that the correlation time and non-Gaussian feature of the noise work in a cooperative way in tuning the performance of noise induced oscillations. Stochastic normal form analysis is performed and the results agree quite well with the simulations. In addition, the theoretical analysis provide us a global view on how non-Gaussian noise functions in the vicinity of Hopf bifurcation. This work may be of interest to a wide readership since oscillations are of ubiquitous importance in many physical, chemical and biological systems.

Acknowledgement

This work is supported by the National Science Foundation of China (Grant Nos. 20933006 and 20873130).

References

- [1] L. Gammitoni, P. Hänggi, P. Jung, F. Marchesoni, Stochastic resonance, *Rev. Modern Phys.* 70 (1998) 223–287.
- [2] B. Lindner, J. Garcia-Ojalvo, A. Neiman, L. Schimansky-Geier, Effects of noise in excitable systems, *Phys. Rep.* 392 (2004) 321–424.
- [3] F. Sagués, J.M. Sancho, J. Garcia-Ojalvo, Spatiotemporal order out of noise, *Rev. Modern Phys.* 79 (2007) 829–882.
- [4] R. Benzi, A. Sutera, A. Vulpiani, The mechanism of stochastic resonance, *J. Phys. A* 14 (1981) L453–L457.
- [5] R. Benzi, A. Sutera, A. Vulpiani, Stochastic resonance in the Landau–Ginzburg equation, *J. Phys. A* 18 (1985) 2239–2245.
- [6] G. Hu, T. Ditzinger, C.Z. Ning, H. Haken, Stochastic resonance without external periodic force, *Phys. Rev. Lett.* 71 (1993) 807–810.
- [7] X. Pei, K. Bachmann, F. Moss, The detection threshold, noise and stochastic resonance in the Fitzhugh–Nagumo neuron model, *Phys. Lett. A* 206 (1995) 61–65.
- [8] A.S. Pikovsky, J. Kurths, Coherence resonance in a noise-driven excitable system, *Phys. Rev. Lett.* 78 (1997) 775–778.
- [9] Z. Hou, T. Rao, H. Xin, Effects of internal noise for rate oscillations during CO oxidation on platinum surfaces, *J. Chem. Phys.* 122 (2005) 134708.
- [10] Y. Gong, Z. Hou, H. Xin, Internal noise stochastic resonance in NO reduction by CO on platinum surfaces, *J. Phys. Chem. A* 109 (2005) 2741–2745.
- [11] H. Li, Z. Hou, H. Xin, Internal noise stochastic resonance for intracellular calcium oscillations in a cell system, *Phys. Rev. E* 71 (2005) 061916.
- [12] V.A. Makarov, V.I. Nekorkin, M.G. Velarde, Spiking behavior in a noise-driven system combining oscillatory and excitatory properties, *Phys. Rev. Lett.* 86 (2001) 3431–3434.
- [13] R.E.L. DeVille, E. Vanden-Eijnden, C.B. Muratov, Two distinct mechanisms of coherence in randomly perturbed dynamical systems, *Phys. Rev. E* 72 (2005) 031105.
- [14] D. Nozaki, D.J. Mar, P. Grigg, J.J. Collins, Effects of colored noise on stochastic resonance in sensory neurons, *Phys. Rev. Lett.* 82 (1999) 2402–2405.
- [15] K. Wiesenfeld, D. Pierson, E. Pantazelou, C. Dames, F. Moss, Stochastic resonance on a circle, *Phys. Rev. Lett.* 72 (1994) 2125–2129.
- [16] C. Tsallis, Possible generalization of Boltzmann–Gibbs statistics, *J. Stat. Phys.* 52 (1988) 479–487.
- [17] E.M.F. Curado, C. Tsallis, Generalized statistical-mechanics – connection with thermodynamics, *J. Phys. A* 24 (1991) L69–L72.
- [18] E.M.F. Curado, Correction, *J. Phys. A* 24 (1991) 3187.
- [19] E.M.F. Curado, Correction, *J. Phys. A* 25 (1992) 1019.
- [20] F.J. Castro, M.N. Kuperman, M. Fuentes, H.S. Wio, Experimental evidence of stochastic resonance without tuning due to non-Gaussian noises, *Phys. Rev. E* 64 (2001) 051105.
- [21] M.A. Fuentes, R. Toral, H.S. Wio, Enhancement of stochastic resonance: the role of non Gaussian noises, *Phys. A* 295 (2001) 114–122.
- [22] M.A. Fuentes, H.S. Wio, R. Toral, Effective Markovian approximation for non-Gaussian noises: a path integral approach, *Phys. A* 303 (2002) 91–104.
- [23] M.A. Fuentes, C.J. Tessone, H.S. Wio, R. Toral, Stochastic resonance in bistable and excitable systems: effect of non-Gaussian noises, *Fluct. Noise Lett.* 3 (2003) L365–L371.
- [24] H.S. Wio, R. Toral, Effect of non-Gaussian noise sources in a noise-induced transition, *Physica D* 193 (2004) 161–168.
- [25] S. Bouzat, H.S. Wio, Current and efficiency enhancement in Brownian motors driven by non Gaussian noises, *Eur. Phys. J. B* 41 (2004) 97–105.
- [26] S. Bouzat, H.S. Wio, New aspects on current enhancement in Brownian motors driven by non-Gaussian noises, *Phys. A* 351 (2005) 69–78.
- [27] P. Majee, G. Goswami, B.C. Bag, Colored non-Gaussian noise induced resonant activation, *Chem. Phys. Lett.* 416 (2005) 256–260.
- [28] D. Wu, X. Luo, S. Zhu, Stochastic system with coupling between non-Gaussian and Gaussian noise terms, *Phys. A* 373 (2007) 203–214.
- [29] G. Goswami, P. Majee, P.K. Ghosh, B.C. Bag, Colored multiplicative and additive non-Gaussian noise-driven dynamical system: mean first passage time, *Phys. A* 374 (2007) 549–558.
- [30] D. Wu, S. Zhu, Stochastic resonance in a bistable system with time-delayed feedback and non-Gaussian noise, *Phys. Lett. A* 363 (2007) 202–212.
- [31] S.E. Mangioni, H.S. Wio, A random walker on a ratchet potential: effect of a non Gaussian noise, *Eur. Phys. J. B* 61 (2008) 67–73.
- [32] Y. Gong, Y. Xie, Y. Hao, Coherence resonance induced by non-Gaussian noise in a deterministic Hodgkin–Huxley neuron, *Phys. A* 388 (2009) 3759–3764.
- [33] Y. Gong, Y. Xie, Y. Hao, Coherence resonance induced by the deviation of non-Gaussian noise in coupled Hodgkin–Huxley neurons, *J. Chem. Phys.* 130 (2009) 165106.
- [34] Z. Hou, T. Xiao, H. Xin, Internal noise coherent resonance for mesoscopic chemical oscillations: a fundamental study, *Chem. Phys. Chem.* 7 (2006) 1520–1524.
- [35] T. Xiao, J. Ma, Z. Hou, H. Xin, Effects of internal noise in mesoscopic chemical systems near Hopf bifurcation, *New. J. Phys.* 9 (2007) 403.
- [36] J. Ma, T. Xiao, Z. Hou, H. Xin, Coherence resonance induced by colored noise near Hopf bifurcation, *Chaos* 18 (2008) 043116.
- [37] J. Ma, Z. Hou, H. Xin, Control coherence resonance by noise recycling, *Eur. Phys. J. B* 69 (2009) 101–107.
- [38] P.H. Coulet, C. Elphick, E. Tirapegui, Normal form of a Hopf bifurcation with noise, *Phys. Lett. A* 111 (1985) 277–282.
- [39] N.S. Namachchivaya, Y.K. Lin, Method of stochastic normal forms, *Internat. J. Non-Linear Mech.* 26 (1991) 931–943.
- [40] L. Arnold, N.S. Namachchivaya, K.R. Schenk-Hoppe, Toward an understanding of stochastic Hopf bifurcation a case study, *Internat. J. Bifur. Chaos* 6 (1996) 1947–1975.
- [41] A. Juel, A. Darbyshire, T. Mullin, The effect of noise on pitchfork and Hopf bifurcations, *Proc. R. Soc. Lond. A* 453 (1997) 2627–2647.
- [42] L. Arnold, P. Imkeller, Normal forms for stochastic differential equations, *Probab. Theory Relat. Fields* 110 (1998) 559–588.
- [43] A. Roberts, Normal form transforms separate slow and fast modes in stochastic dynamical systems, *Phys. A* 387 (2008) 12–38.
- [44] L. Arnold, X. Kedai, Normal forms for random differential equations, *J. Differential Equations* 116 (1995) 484–503.
- [45] J.B. Roberts, P.D. Spanos, Stochastic averaging: an approximate method of solving random vibration problems, *Internat. J. Non-Linear Mech.* 21 (1986) 111–134.
- [46] P.H. Baxendale, Stochastic averaging and asymptotic behavior of the stochastic Duffing–van der Pol equation, *Stochastic Processes Appl.* 113 (2004) 235–272.